ULTRALIGHT FRP PSEUDOSPHERICAL SHELL

G.L.Narasimham [1] and R.Ramesh Kumar [2]

[1] ***Composites Group, Vattiyoorkavu, Vikram Sarabhai Space Center,Trivandrum 695013,India***

[2] ***Structural Engg Group, VRC, Vikram Sarabhai Space Center,Trivandrum 695022,India***

SUMMARY: A structural synthesis is made for FRP shell structure that does not buckle under axial load, and is stable up to compressive failure. A multi layer shell construction with defined non-geodesic filament orientation and shell wall thickness is determined. From equilibrium and stability requirements the shell surface turns out to be warped or to possess negative Gauss curvature K. They have zero normal curvature for the directions in which reinforcements run. The definition of isometric deformation is seen as shell bending. Hyperbolic geodesics introduced in this paper are in accordance with Gauss Egregium Theorem and are seen essential to the structural stability of thin walled shells. It is viewed as a stability criterion. Generalized Mohr's circles are drawn to depict changes in curvature during isometric bending. Initially finite element analysis of reticulated pseudospherical shell is carried out. A multi-layered FRP shell made of high modulus graphite composite has high resistance to buckling ,with stress at buckling highest so far obtained. The design of pseudosphere derived from static equilibrium and stability defined here is independant of length to maximum diameter ratio This size independance is theoretically built into synthesis and as well verified by analysis.

KEYWORDS: Bending, Isometric invariance, Theorema Egregium, Hyperbolic geodesics, Negative Gauss curvature, Asymptotic directions, Pseudosphere, non-Euclidean hyperbolic geometry ,Generalized Mohr's circle for isometric bending, Tschebycheff net,inverse isometry.

1. INTRODUCTION :

When glass bottles break, bottlenecks are almost intact. Spinal cord bones have a narrow waist, same shape prevails from big thigh bone to smaller phalanges of hand or toe. Nylon shopping net bags and fishing nets assume a warped surface in free areas when loaded, filaments having no normal curvature on net surface. Soap bubble films freely drawn between two rings exhibit a negative curvature by membrane tension. A flat strip becomes stiffer after twisting it plastically into a helicoid. These and several such examples make one ponder that , after all, there could be some natural economy in material usage in such shapes for optimally balancing buckling instability which gets triggered as bending at elemental structural level.

2.1 Structural Synthesis of shells:

The method incorporates the geometrical basis of bending in classical surface theory in differential geometry in an attempt to establish it for removing bending that causes buckling instability. It emphasizes not what varies, viz. normal curvature, but what does not vary viz. geodesic curvature k_g and Gauss curvature K, for .incorporation as essential structural objects obtaining geometric nonlinearity and large deformation advantages

2.2 Design of filamentary axisymmetric pressure vessels

This is briefly reviewed, as similar synthesis procedure is used. We consider a doubly curved differential shell element. Fig (1).

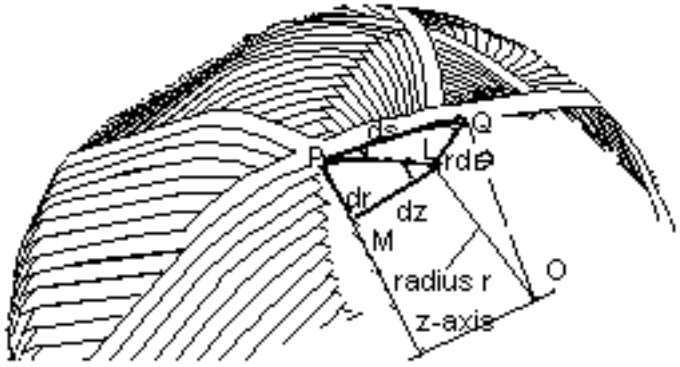

FIG 1. DIFFERENTIAL SHELL ELEMENTS FOR A DOUBLY CURVED FILAMENT WOUND SHELL OF REVOLUTION

FILAMENT NORMAL CURVATURE POSITIVE FOR PRESSURE LOAD AND ZERO FOR NO LOADING

Here winding angle LPQ=ψ and angle PLM=ϕ , slope of meridian.

Pressure equilibrium normal to shell $N_{|}/R_1 + N_o/R_2 = p$ (1)

Membrane stress resultants $N_\phi = pR_2/2$, $N_\theta = pR_2(1 - R_2/2R_1)$ (2)

Here p is the pressure, N_ϕ, N_θ are the stress resultants along meridional and hoop directions, R_1 and R_2 are principal radii of curvature . We employ netting theory. Although from an analysis viewpoint netting theory is held to be to too general or simplistic, from a synthesis viewpoint it has some advantages. It captures the essential directed load bearing reinforcements, their size and direction, discarding the negligible shear contribution of resin. Netting theory directly depicts a pure membrane and funicular state of stress of a single balanced layer that lends itself to imposition of appropriate stability criterion and uniform stress by simple static equilibrium.

If N_S is the stress resultant along fiber arc s and ψ the winding angle between filament and meridian,

$N_\phi = N_S \cos^2\Psi$, $N_\theta = N_S \sin^2\Psi$, $N_\theta / N_\phi = \tan^2\Psi$ (3)

Combining Equns (2) and (3) we have $R_2/R_1 = 2 - \tan^2\Psi$ (4)

To define winding angle Ψ, we employ geodesics in filament winding which have zero geodesic curvature or curvature in the tangential plane given by Liouville's formula for surfaces for revolution. These are zero slip stable lines suitable for normal to the laminate pressure loading and processing by filament winding.

$k_{gE} = +d\Psi/ds + \sin\phi \sin\Psi / r = 0$ (5)

On integration we get $r.\sin\Psi = r_{OE} = \text{constant}$ (6)

This is Clairaut's Law for geodesics on surfaces of revolution. Here, r is the shell radius. The subscript E, stands for elliptic, explained later . Shortest lines on convex surfaces eg. great circles on spheres and helical lines on cylinders are examples. Combining Equns (4) and (6) we obtain required shapes and filament orientations for the "geodesic

isotensoid ” in terms of elliptic functions. Same cross sectional area of filament rovings running between equator to boss opening radius r_{OE} is used and this yields constant stress along filaments. Sufficiently large number of layers are chosen to isolate bending from stretching. We can employ any other type of geodesic in structural synthesis.

We employ the above derivation for synthesis of an axisymmeric shell loaded between two parallel circles. No normal pressure or loading acts. We introduce axial loads *through* the skin so that direct bending of the laminated shell by a normal load component is avoided .The loads are transmitted through the shell onto the other end. From Equn (1), normal pressure p acting on the differential element is zero. Introducing Equn (3) into (1) and , letting $k_1 = 1/R_1$, $k_2 = 1/R_2$, we have $k_1 \cos^2\Psi + k_2 \sin^2\Psi = 0$ (7)

This is the Euler expression for normal curvature of a filament k_n on a doubly curved shell that vanishes in this case unlike the geodesic-isotensoid . Zero normal curvature lines are called *asymptotic lines*. Examples of asymptotic lines on some surfaces are:

(a) A typical saddle point Fig (2). . Parametric representation (x,y,z) = f(u,v)

x= u cos v, y= u sin v, z= C.sin 2v.The second surface in Fig (2) has inflexion points at center and such a surface was fabricated by Beltrami [1]

FIG 2 WARPED SURFACES . FIRST ONE IS A SIMPLE SADDLE SURFACE . SECOND ONE HAS FIVE HUMPS AND A SIMILAR ONE WAS MADE BY BELTRAMI. WITH THREE HUMPS IT IS A MONKEY SADDLE.

(b) Straight skewed generators on a one sheet hyperboloid of revolution,

$r^2 - z^2\tan^2\alpha = a^2$, x =a tan$\infty$, y=a, z = a tanθ/tanα, α is inclination between generator and z-axis.; r and θ are parameters

(c) *Hypar* or hyperbolic paraboloid surface $2z = x^2/a^2 - y^2/b^2$; $x/a \pm y/b$ = constant, are generators, set of parallel line projections inclined at $\tan^{-1}(b/a)$ to x- axis. Parametric representation (x,y,z) = f(u,v) is

x = a (u+v) ; y = b(u-v) ; z = 2uv;

(d) Curved asymptotes with constant winding angle 45^0 to the principal curvature directions on a catenoid of revolution; r = C cosh (z/C) , where C is the minimum distance of catenary to z-axis of symmetry. This holds for all surfaces of zero mean curvature or minimal surfaces which are physically seen as soap bubble films possessing no bending rigidity .

3.1 Hyperbolic curvature and hyperbolic geodesics

Liouville’s formula ([2],pp154) for geodesic curvature is given by

$k_{gE} = + d\Psi/ds + \cos\psi\,(k_g)_{v=const} + \sin\psi\,(k_g)_{u=const}$ (8)

where right hand side k_g are functions of E,F,G and their derivatives with respect to parameters u and v of first fundamental form introduced later.

In polar coordinates for axisymmetry, $+ d\Psi/ds + \sin\phi\ \sin\Psi / r = 0$ for geodesics

Integrating this we get $r.\sin\psi = r_{oE}$=constant, which are straight lines.

In this paper we define hyperbolic curvature by simply changing the sign of ψ in Equn (8),and justify such a change from inversion

$k_{g\ E,H}$= ± dψ /ds + sinϕ sinψ/r =0 (+ for Elliptic, - for Hyperbolic)

k_{gH}= - dΨ/ds + sin ϕ sinΨ / r = 0

Integrating this we get r/sin ψ=r_{oH}=constant, circles through origin (9)

This is also obtained by putting r in place of $r_{oE}.r_{oH}/r$ as a process of inversion of complex variable conformal transformation w=1/z .We represent in Fig (3) both the types of geodesics in two dimensions.. Rectilinear triangle abc in elliptic model is inverted to curvilinear triangle ABC in a hyperbolic model. The sense of rotation is changed .Radius

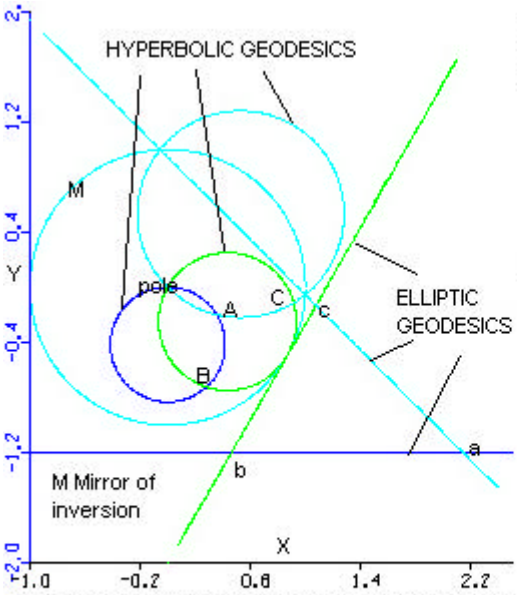

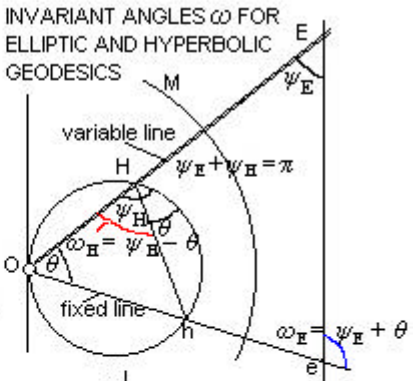

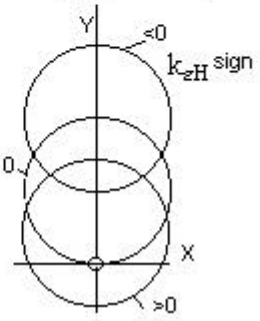

FIG3.Triangles ABC and abc have "straight" sides in hyperbolic and elliptic geometries.Angles at A,a B,b C,c are equal in this inversion,but sense is reversed

of circle or mirror of inversion =$(ro_H.ro_E)^{1/2}$ .and ❺$_E$ ⑥ -❺$_H$

.It is difficult to accept the hyperbolic model in two dimensions as there is no Euklidean counterpart ([3],pp 275).The definition of geodesic curvature is dependant only on the coefficients of the first fundamental form and is an intrinsic bending invariant property in either case.

Also the metrics of the above cases in two dimensions are:

$ds^2=dr^2+(rd\theta)^2$ and $ds^2=[dr^2+(rd\theta)^2]/r^4$, inverted to a unit circle.

Arc lengths should be extremized in each case to be a geodesic We use Euler-Lagrange equation in Calculus of variations approach.

Functional in each case is $F= (r^2+r'^2)^{½}$ and $F= (r^2+r'^2)^{½}/r^2$

When F is independent of θ , F-r'∂F/∂r'=constant . Performing the integration for Euclidean/Elliptic case we have r sinψ= constant =r_{oE}. Likewise for hyperbolic case we get r/sinψ= constant= r_{oH}.

As ds = rdθ /sinψ we have (sinϕ ± dψ/dθ)=0 ; Integrating ψ±θ sinϕ = ω (10)

where arbitrary constant ω is the constant angle turned in the tangent plane.

For flat Euklidean geometry ϕ =π /2 , ❻=❺ ± θ (11)

All angles are consistently measured counterclockwise positive, from radius vector towards elliptic/hyperbolic arcs. In elliptic geodesic,❻$_E$ constancy means that ❺+ঌ is the same angle for the straight line Ee in Fig (3),right. In hyperbolic geodesic,❻$_H$

constancy means that ❺-ৎ is the same angle contained in the "straight line" segment OHh .

3.2 Elliptic and Hyperbolic curvature of a circle in two dimensions

Constant elliptic/euklidean curvature forms a circle. We look at a curve of constant hyperbolic curvature defined here.

For a circle in two dimensions in x-y plane we have relations

$\sin \psi / r = (1-T^2/r^2)/2a$; $d\psi/ds = (1+T^2/r^2)/2a$; $T^2=h^2-a^2$ (tangent squared or power) (12)

adding and subtracting $k_{gE}=1/a$; $k_{gH}= (a-h^2/a)/r^2$ (13)

Curvatures in polar coordinates are expressible as (primes with respect to θ)

$k_{gE}=(r^2 +2r'^2 - rr'')/(r^2 + r'^2)^{3/2}$; $k_{gH}=r\,(r+r'')/(r^2 + r'^2)^{3/2}$ (14)

which have geodesic solutions $r=r_{oE}\sec(\theta+\alpha)$ and $r=r_{oH}\cos(\theta+\alpha)$,0 (15)

where r_{oH}, r_{oE},α , are all easily recognizable constants in Fig (3)

Thus k_{gE} is independent of position , Hyperbolic curvature is position dependent for an arc of a circle. It is positive, zero or negative depending on whether the origin is enclosed, lies on the rim or outside the circle. Fig (3),right.. Some curves of constant positive and negative k_{gH} are given in Fig (4) for same boundary conditions.

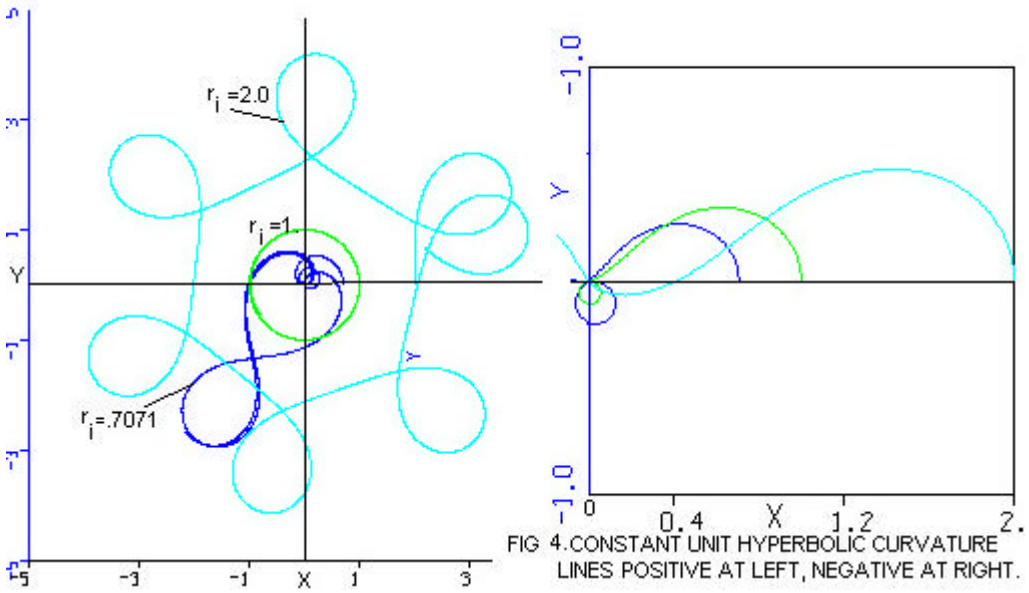

FIG 4.CONSTANT UNIT HYPERBOLIC CURVATURE LINES POSITIVE AT LEFT, NEGATIVE AT RIGHT.

3.3 Justification to consider vanishing k_{gH} as geodesics in this paper

First justification for considering these hyperbolic lines as geodesics comes from an application of Gauss-Bonnet Theorem [2],[3] considered for both cases.

° $k_{gE\ or\ H}$ ds + ° ° KdA +☒ (π -ↀ) =2 π

Hazzidakis theorem ([2],pp 204,prob 17 and [3],pp237, prob 15).deal with a variant of Gauss-Bonnet theorem. The area of a *quadrangle* enclosed between four elliptic geodesic arcs is (angle sum- 2π) or twice the spherical excess of a geodesic triangle. By the theorem of Hazzidakis when this is formed between *lines on constant negative K* can be regarded also as another type of geodesics. Secondly, this has also been demonstrated by Beltrami,([2],pp152) but with reported difficulties at edge of regression or cuspidal equator.Thirdly, asymptotic lines on constant negative K are found to form a Tschebycheff net, the same result arrived at by incorporating present hyperbolic geodesics.[2],(pp204,prob 15).Fourthly, following article 5.3 demonstrates that Egregium Theorem as asymptotic lines on constant negative K, the same equals (2π -angle

sum). Thus asymptotic a stability theorem of bending invariance only on the assumption of validity of the hyperbolic geodesics. The fifth justification comes from a simple experiment with a nylon shopping bag,like one in Fig(8) bottom. .It has knots on it at regular filament spacing and assumes a definite shape on loading. The distance between nodes ds and polar separation dψ of rhombic cells are constant by knitted construction of vented bags. Thus, ds/dψ is a constant. This for each cell or differential shell element equals r/sinθ. On flattening the bag to draw filaments to center,they arrange themselves as circles passing through the center with constant radius r/sinθ=r_{oH}. It is noticed that after a small load, filament stress transmitted through the knots increases *in that stable configuration*, large bending deformations having stopped in proportion. The stable shape is from a pseudosphere family, shown later.

4.1 Models of hyperbolic geometry

There are 3 models of hyperbolic geometry due to Klein, Poincaré and Beltrami. The present model is nearest to Beltrami model in which there appears a limitation for drawing geodesic triangles near to the cuspidal edges. In Fig (5) and Table 1 present model is compared with Poincaré model.

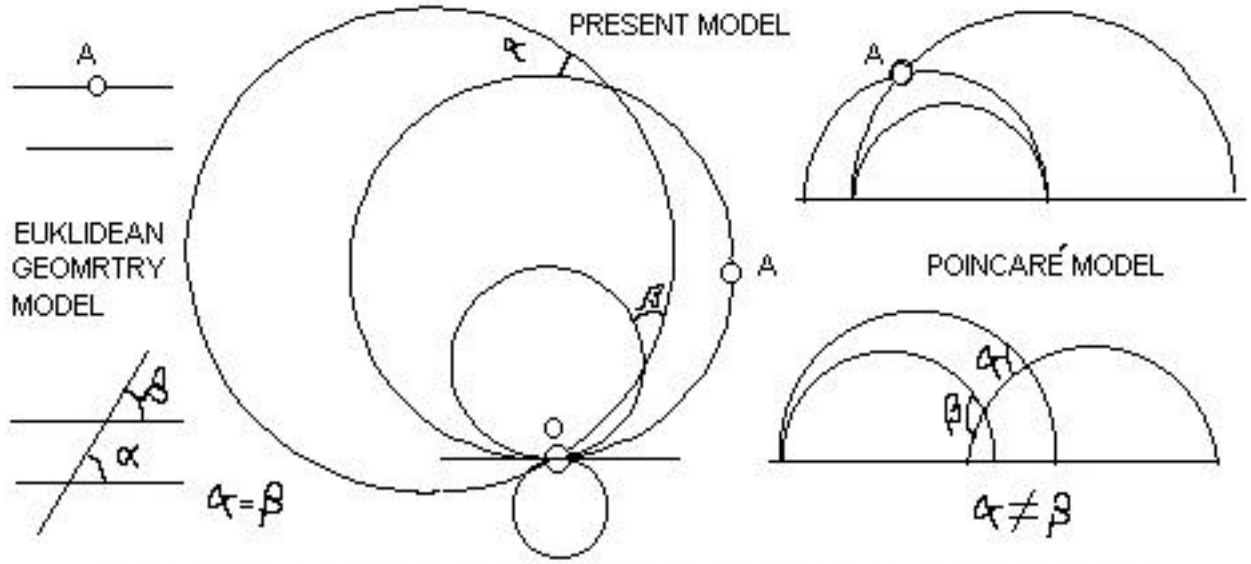

FIG 5. HYPERBOLIC GEODESICS DO NOT CONFLICT WITH EUKLIDEAN GEOMETRY

.***Table 1 Comparison of hyperbolic geometry models in two dimensions***

Euclidian /Elliptic model	Poincaré model	Present Polar model
Geodesic is a straight line	Geodesic is a semi circle	Geodesic is a full circle through origin
Lines go to infinity if continued on either side	Lines go to x axis if continued	Lines go to origin if continued
Points at infinite distance are indefinite	Points at infinite distance are on the x axis	Points at infinite distance are at the origin
Only one straight line possible through any two points	Only one semi circle possible between any two points	Only one circle through any two points. The third point is the origin.
Two straight lines are parallel if they have a common point	Two semicircles touching the x axis are parallel although intersecting	Two full circles are parallel if they have a common tangent at origin

at infinity		
Only one line parallel to a given line through outside point	Two semi circles possible as parallels from an outside point with common semicircle tangency.	Only one full circle possible to a given circle with common tangent at origin
If a line intersects two parallel lines, the alternate angles are equal	The alternate angles got by cutting two parallel semi circles are *not* equal	When a circle intersects two parallel circles alternate angles are equal
Metric$ds^2=dx^2+dy^2$ Or $ds^2= dr^2+(rd\theta)^2$	Metric $ds^2 = (dx^2+dy^2)/(y/a)^2$	Metric $ds^2 = (dr^2+(rd\theta)^2)/(r/a)^4$
Physical analogy is a light ray with constant speed	Physical analogy light ray with speed proportional to y coordinate	Physical analogy light ray with speed proportional to square of radial distance from origin
Sum of three internal angles is π	Sum of three internal angles can be anything	Sum of three internal angles is π
Inversion of hyperbolic model	bilinear transformation of complex variable conformal mapping	Inversion of elliptic model

5.1 Generalized Mohr's circle of curvatures in isometric bending for positive and negative K.

It is possible to depict normal and twist curvatures on the familiar Mohr circle. This has been done in a comprehensive way, accommodating isometric bending in this paper.

Zero normal curvature direction can occur only on negative K surfaces demarcating positive and negative normal curvature areas .This is represented on the Mohr's circle using power of co-axal circles Fig (6) to include all possibilities by isometric bending .

On x-axis is normal curvature and on y-axis twist curvature (or geodesic torsion τ_g in differential geometry parlance) is drawn. Geometrically, the square of semichord or tangents from origins equals of product of intercepts of principal curvatures. As the shell or laminate gets bent to larger values of k1/k2 with K=k1.k2 remaining constant as per Egregium theorem, a new Mohr circle takes over, at a common point without changing twist curvature or τ_g. At any instant ψ equals $\tan^{-1}(-k1/k2)^{1/2}$.The same is shown for positive K in.Fig (6).

There is equal tangent length for all circles. Square root of Gauss curvature is represented by common τ_g intercept for all circles with negative K and as equal length tangent drawn from origin for all circles with positive K. Three circles at left represent negative, zero and positive $K=T^2$ of Equn (12). As per [3], pp 276-279, these geodesics are orthogonal to a group of motions in plane hyperbolic geometry. Case of K=0 is coinciding with the choice made in the paper.

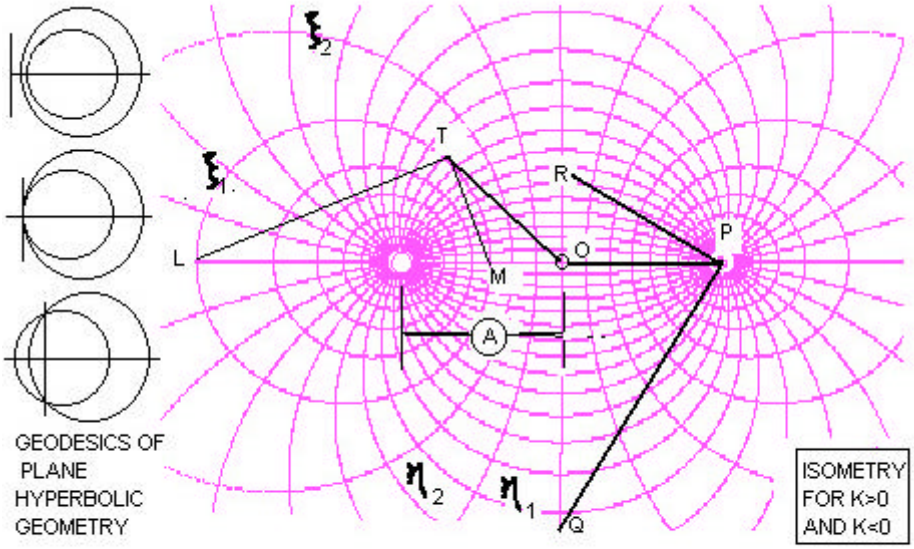

FIG 6. FOR CO-AXAL SYSTEM OF CIRCLES, GAUSS CURVATURE INVARIANCE IS SEEN WHEN K>0 OT.OT=OM.OL COMMON TANGENT AND WHEN K<0 OP.OP=OQ.OR COMMON SEMI CHORD REPRESENT SQUARE OF A , SAME FOR ENTIRE DIAGRAM. FLEXURE POTENTIAL ξ FOR K>0 AND DISTORTION FUNCTION η FOR K<0 DEPICT GENERALISED MOHR'S CURVATURE CIRCLES

Physically, this can be demonstrated using a flexible hollow spherical rubber ball cut into two equal hemispheres. Diametrically opposite points of each half are squeezed together, bent and rolled in until it assumes a spindle shape of same constant K. The surface is isometrically deformed, that is to say, on application of bending and twisting moments, there is no stretching or shear strain in the mid surface of its round wall.

Although not so readily apparent, this holds also in bending of negative K sheets of flexible material. Several books on differential geometry deal with isometric mapping and first fundamental form equivalence between catenoid and helicoid, eg., [2], page 121. By a series of bend-twist operations a catenoid can be deformed to a heliciod and vice versa. Take a flexible catenoid , cut it along a meridian and apply simultaneously bending and twisting moments until the nearest circle r = C becomes the straight twisted spine of helicoid . Meridians looking away from center now align straight in the manner of motion of aircraft propeller blades cutting through air in flight. Before bend-twisting principal curvatures were at $0,90^0$ and asymptotes along $\pm 45^0$ After bend-twisting, principal curvatures are along $\pm 45^0$ and asymptotes at 0,90 degrees ,ie., there is a swap between the two directions. However, at any point K remains the same. This example is classical, gives an initial mistaken impression that mean curvature H=0 remains the same in isometry, as both the catenoid and helicoid are minimal surfaces. It is not invariably so . The textbooks on differential geometry that could be accessed by the author do not give isometrically twisted helical surface equivalents to the pseudosphere set, perhaps as it is easiest to calculate surfaces of revolution.. But it can be calculated from Equn. (30) that follows after suitable u,v parameterization is assumed.

5.2 Isometry depiction using Flexure Potential and Distortion Function

The above bending phenomenon can be even more systematically depicted by using a complex variable isometry function w for any curved surface. Let $1/a = (abs(K))^{½} = A$, where a is the cuspidal radius of pseudosphere or spherical radius in case of constant K.

$z=A \coth(w/2)$ or $w = \ln [(A+z)/(A-z)] = (\xi + i \omega)$ where complex curvature $z=k_n+i\,\tau_g$ (16)

ξ circles are : $(x-A \coth \xi)^2 + y^2 = (A/\sinh \xi)^2$ (17)

ω circles are : $(x+A \cot \omega)^2 + y^2 = (A/\sin \omega)^2$ (18)

from which circle center locations and circle radii are obtained. The ξ circles are Apollonius circles with respect to poles, $\xi=\ln(r_1/r_2)$,where r_1 and r_2 are distances from points on Mohr circle to the poles. The ω circles contain constant angle ω_1 on the inter-pole chord.

Gauss theorem or other literature in isometry does not identify what varies in isometry *as a single geometrical parameter f*or each Mohr circle at any stage of bending deformation. For this purpose, the author introduces the above ξ and ω as Flexure potential and Distortion function respectively, taking a cue from electrostatics and fluid dynamics. In the former there is electrical

flow between oppositely charged poles, and in the latter, streamlines between source and sink in irrotational flow. We have potential and stream functions ξ and ϖ analogous to bending deformation in a phenomenon. K being positive or negative is observed even in curvature of Space [8],where it is observed as relative "strain" of circumferentially surrounding matter.

We begin bending a synclastic spherical surface starting with equal curvatures until one curvature becomes too large compared to the other. This is represented by a pole growing towards y-axis as a Mohr circle with same tangent length equaling $K^{1/2}$.=1/a =A .Each Mohr circle has a value $\xi=\xi_1$; The principal curvatures are :

k_1= A. tanh (ξ_1 /2) and k_2= A coth (ξ_1 /2), where $\xi_1 = 2\,[th^{-1}(k_1/k_2)^{1/2}]$ (19)

Similarly we bend a saddle point with curvatures equal but opposite signs eg., soap bubble film saddle point. This is represented by a circle of radius A with center as origin. As we squeeze the laminate, the circle co-axially travels up or down, center remaining on y-axis, always passing through the poles and retaining the same semi chord length A = 1/a. Each Mohr circle has a value $\varpi = \varpi_1$,

$-k_1$=A tan (ϖ_1/2) and k_2= A cot (ϖ_1/2) , $\varpi_1 = 2\,[\tan^{-1}(-k_1/k_2)^{1/2}] = 2\psi$ at pole. (20)

These are depicted on a bipolar grid in Fig.(6).Complex curvature w can be slightly altered to include ⑤ =0 for $k_1=k_2$ unbent state, but it is not included here .We see that ξ -ϖ space above belongs to inextentional isometric deformation *implied* in text books of differential geometry.

The theorem of Beltrami-Enneper states that the twist curvature of a line on a given negative K surface or geodesic torsion is simply $\sqrt{(-K)}$, K need not be constant on the surface. Since the twist curvature is same, Mohr circle of every bent laminate must pass through this point.

A structural analysis to find strains and stress even on an isotropic material cut catenoid involves high geometric nonlinerarity on the scale of topology of flexible rubber membranes. It would indeed be an interesting problem to prescribe the right magnitude of bending and twisting moments in modeling of the static problem with rotating forces along the edges, leaving K the same at every load increment This problem would be a fine example of pure bending as per notions of inextensional bending and isometry introduced by Gauss, Beltrami, Bour and Minding, when large deformation stress and deformation is computed for every increment of ⑤ or ϖ

5.3 Incorporation of hyperbolic geodesics into equilibrium

From Equn (7) and (9) we get $d\phi/(dr/\sin\phi)/(\cos\phi/r) = \tan^2\psi = r^2/(r_{oH}^2-r^2)$

Integrating, $\cos^2\phi = (r_{oH}^2-r^2)/a^2$, where a is a new arbitrary but important constant. (21)

differentiating the above, we get $d\phi/(dr/\sin\phi)\,.\,(\cos\phi/r) = -1/a^2$, or $\mathbf{k_1k_2 = K = -1/a^2}$

we split r_{oH} into two factors a and μ , to designate μ as a dilation factor between maximum cuspidal radii of each pseudosphere of constant μ value. $r_{oH} = a\,\mu$ (22)

From (21) and (22) we get $\cos\phi = [\mu^2 - (r/a)^2]^{1/2}$ (23)

From (23) and (9) we get $\cos\phi/\cos\psi = \mu$ (24)

Solving the equations $k_1\,k_2=-1/a^2$, $k_1/k_2= -\tan^2\psi$ from Equn(7) we get

$k_1=-\tan\psi/a$, $k_2=\cot\psi/a$; intrinsic curvature equations of pseudosphere at any ❺ (25)

Eliminating ϕ between (7), (23) we get back $\sin\psi/r = 1/(a\,\mu) = 1/r_o$ (9).

Likewise, it is possible to show that when constant K and hyperbolic geodesics are given, one arrives at asymptotic lines.

Thus, assumption of the above hyperbolic geodesics with asymptotic character leads to a constant negative K as our solution. The result coincides with Theorema Egregium. which states that this scalar is bending invariant. Hence, the constructed hyperbolic geodesics are valid isometric invariants and are more important in specifying direction in fibrous composite design as Gauss curvature K. A pseudosphere with meridional and hoop reinforcements is a wrong choice in filament direction.

For central pseudosphere μ = 1, a closed form solution is

$\phi = \psi$, $r = a\,\mathrm{sech}\,\theta = a\sin$ ❷ , $z = a\,(\theta - \tanh\theta)$, $\sin\psi/r = 1/a$

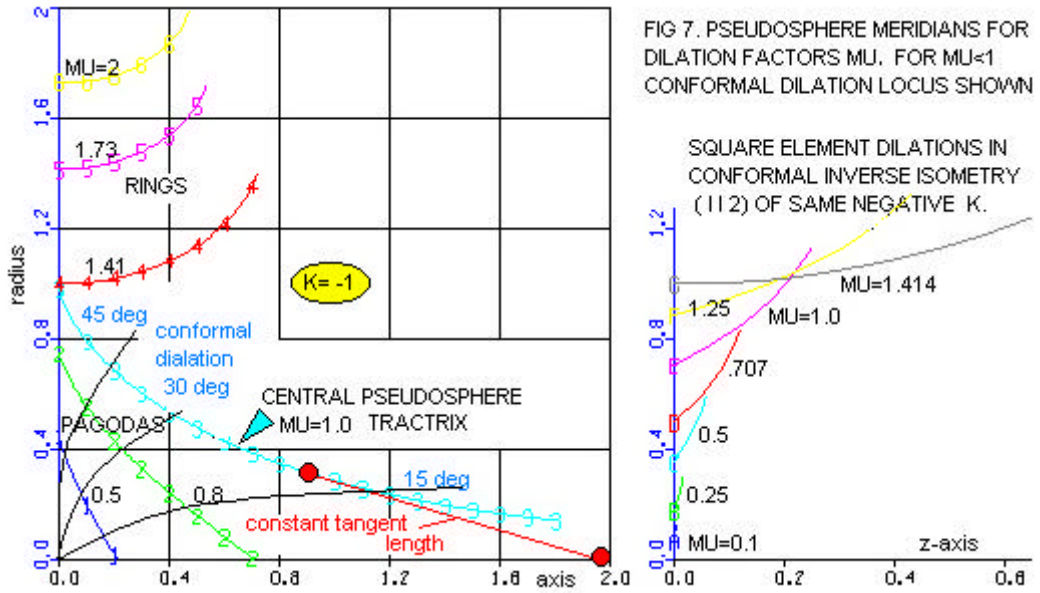

The meridian is a tractrix which has a constant tangent length between point of tangency and z-axis.It is also called pseudoradius([2],pp148). Some meridians are shown in Fig (7) for various values of μ. Except the tractrix all are periodic.ψ is incremeted in equal steps of ⑥/n to obtain a reticulated or discrete model .

The constitutive equations above can be also written :

$(d\psi/ds)^2 + \cos^2\psi / a^2 - 1/r_{oH}^2 = 0$; s=a ③ F(③ ,⑥ /2-❺) ; s=-a .log tan (ψ/2) or ③=1 (26)

and $d^2\psi/ds^2 = K \sin\psi . \cos\psi$; an intrinsic (ψ - s) relation (27)

The synthesis yields a funicular thin-walled shell where load transfer between mutually reinforcing filaments occurs at knots or nodes for a disretized reticulated structure and as interlaminar shear between layers in a continuous balanced shell.

5.4 Tschebycheff net. It is interesting, relevant and useful to find that above equation (27) represents a net with filaments along asymptotic directions of constant negative Gauss curvature K. Surfaces of flexible fishing net having same distance between knots is taken and draped on the surface such that the filaments and knots lie along asymptotic directions with zero normal curvature. An intrinsic relationship Equn (27) between ψ and arc distance fits in exactly as above. Each rhombus distorts by scissoring action to form neighboring cells in the Tschebycheff net. The pseudosphere described in this report are Tschebycheff nets.[2], page 204 prob. 15 for various μ values. Fig (8) shows three pseudosphere types.

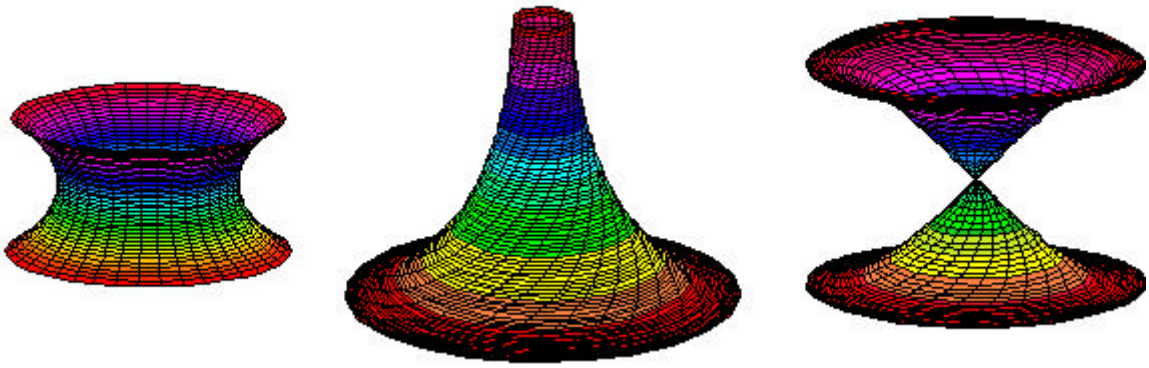

G 8. SURFACES OF CONSTANT NEGATIVE GAUSS CURVATURE. DILATION FACTORS ARE GREATER, QUAL TO OR LESS THAN 1. THE FIRST IS HYPERPSEUDOSPHERE DRAWN WITH LINES OF PRINCIPAL URVATURE,NEXT TWO CENTRAL PSEDOSPHERE AND HYPOPSEUDOSPHERE WITH ASYMPTOTIC LINES

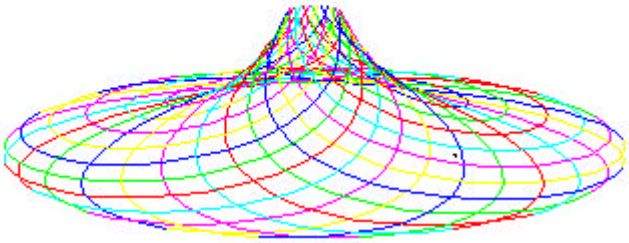

ASYMPTOTIC LINES ON A CONSTANT NEGATIVE GAUSS CURVATURE SURFACE REPRESENTING A TSCHEBYCHEFF NET. NET LINES SHOWN ARE HYPERBOLIC GEODESICS ON THE CENTRAL PSEUDOSPHERE

To design composite shells optimally it is seen that the quotient of principal curvatures Equn (7) is negative, so also is the product K. We should therefore rule out cylinders, cones (K=0 developable surfaces), and synclastic surfaces (K>0) from normal to the shell equilibrium consideration. Only negative K surfaces that too reinforced only along the asymptotic directions. qualify to carry membrane loads. These are saddle shaped points called also anticlastic as curvatures are in opposite directions along principal orthogonal directions.

When the position vector [**r**] is described with respect to parameters u and v, there two fundamental forms in surface theory*:*

I $ds^2 = E\,du^2 + 2F\,du\,dv + F\,dv^2$; (28)

II $k_n\,ds^2 = L\,du^2 + 2M\,du\,dv + N\,dv^2$; (29)

Here we introduce Theorema Egregium . The remarkable theorem states that under isometric or bending deformations, Gauss curvature K is invariant. This had been demonstrated by Gauss. [9]. In the expression for double Gauss curvature

$$K = (LN - M^2) / (EG - F^2), \qquad (30)$$

the numerator has coefficients L,M,N from the second fundamental form of surface theory and is expressible in terms of E,F,G, the coefficients of the first fundamental form and their derivatives with respect to surface generating parameters u and v in a curvilinear coordinate system. The surprising aspect is, the determinant of second fundamental form $LN\text{-}M^2$ getting independent of L,M,N and depending only on E,F,G and their partial derivatives. This justifies intrinsic stability of hyperbolic geodesics in membrane state. Some quantities that remain invariant in isometry or isometric mapping as they depend purely on the first fundamental form are : lengths, winding angle or included angle between arcs, angle turned in tangential plane $\int k_g ds$,$\iint KdA$ or integral curvature (Integra Curvatura as nomenclatured by Gauss), geodesic curvature of two

types, the second type is defined in this paper, Gauss curvature, geodesic torsion, Christoffel symbols. In structural design and analysis parlance we can say that they do not change by inextensional deformations. That is, there is no midplane extensional strain including in-plane shear deformation. The first fundamental form fully covers shell membrane state of stress and strain and the second fundamental form covers the bent state.

Some cosequences of this theorem : (1) Surfaces of positive or negative K cannot be faithfully i.e.,isometrically mapped onto a plane without stretching ε or shear distortion ℘ .When we step on an egg shell making it flat,circumferential cracks appear. It is impossible to map features on the globe on a flat sheet without compromising on inplane strains ε or ℘ .(2) Direct or full isometry is possible among surfaces of same constant K. (Minding's Theorem [2],pp 145).Hence, so long as there is bending, we may have widely varying principal curvatures k_1 and k_2, and external shape but a constant product K , like for example an inverse relationship between pressure and volume of an ideal gas at same temperature.

Gauss theorem is also stated simply as *K is an isometric invariant.* In Fig (9) is seen a netted construction in which for each rhombic cell length is same but not the element angle, apparently a contradiction. Textbooks in differential geometry do not fully illustrate direct and inverse isometry. In inverse isometry the question is asked that if K is same on two surfaces, whether angles *and* lengths have to be the .same. It is in-plane strain and bending of a single differential element that decides partial isometry. This paper defines the two circumstances for which converse requirement is partially fulfilled.. That is, if K is constant in a deformation , it does not necessarily mean that there has been a strict dual (❺-ds) invariant isometric corrospondence, which we can call direct isometry. In bending,k_1=-tan❺/a, k_2=cot❺/a, normal curvature ratio k_1/k_2 changes, K and other quantities from first fundamental form cannot change. We see in above Fig (7) how change in local or differential shell element membrane dimensions can produce global bending of the structure in three ways. In direct isometry (DI), ds ***and*** ❺ are constant ,(e.g., catenoid/helicoid –classical bending). In inverse or partial isometry defined here ***either*** ds ***or*** ❺ is constant. Retaining same rhombic or diamond cell lengths ds through a dilation factor ③ , ❺ changes by scissoring/shearing action of a Tschebycheff net,This is situation (II1) Whereas retaining ❺ conformally, but changing ds (and rotations in principal planes, principal curvatures $k_1$and k_2 remaining same) with magnification or contraction occuring through a dilation factor ③, we have situation (II2).This is shown for a square element (❺ =⑥ /4).It must be noted that *applicability* by making one differential shell element to hug onto another one is possible only in DI mode by bend-twisting, but not in II1 and II2 modes. The latter modes require the element to be dilated or distorted to make element edges and corner nodes to fall one over the partial isometric equivalent during draping action.

.

6.1 K changes by large in-plane circumferential strainingin a circular plate

Gauss Theorem stipulates no midplane straining as long as K is invariant. By implication midplane straining of laminate is associated with change in K. Let us see how this comes about.

Circumferential straining around a flat point is the simplest way to change K. Take a circular disc of radius R , circumferentially strain it to adjust to large deformations Apply a tensile plastic permanent parabolically varying circumferential strain $+Kr^2/6$ by any means. This produces a minimum surface area film saddle surface of radius 1/K in two mutually orthogonal directions, as a potato chip. Refer first of Fig (2). Gauss curvature obtained is negative. Maximum tangential rotations are ± KR, along principal directions. Now instead of tensile we apply compressive strain $-Kr^2/6$, to obtain a segment of a sphere of radius 1/K,maximum tangential rotation or semi-cone angle $\sin^{-1}(KR)$.Thus K that characterizes bulging or warping of a surfaces is a matter of changing hoop strain *in comparision* to radial strain by large deformation Von Kármán *compatibility*, which is neglected in linear formulations. This can be readily demonstrated on flexible honeycomb core made by Hexcel Company ,for example. Fig. (9), right pictures.

Flat metric $ds^2=dr^2+(rd\phi)^2$ is generalised to include circumferential strain ing to a doubly curved shell metric in geodesic polar coördinates as $(r\rightarrow u)$ $ds^2=du^2+(ud\phi)^2(1+Kr^2/3)$ where now u is measured radially along the surface. Constant K axisymmetric meridians of either sign are simply generated by $d^2r/ds^2+Kr=0$ depicting strain around each point. ([2],pp146-149)

6.2 Strip deformation by differential straining

When a long flat strip is twisted to form a helicoid or a part of sphere set, there is

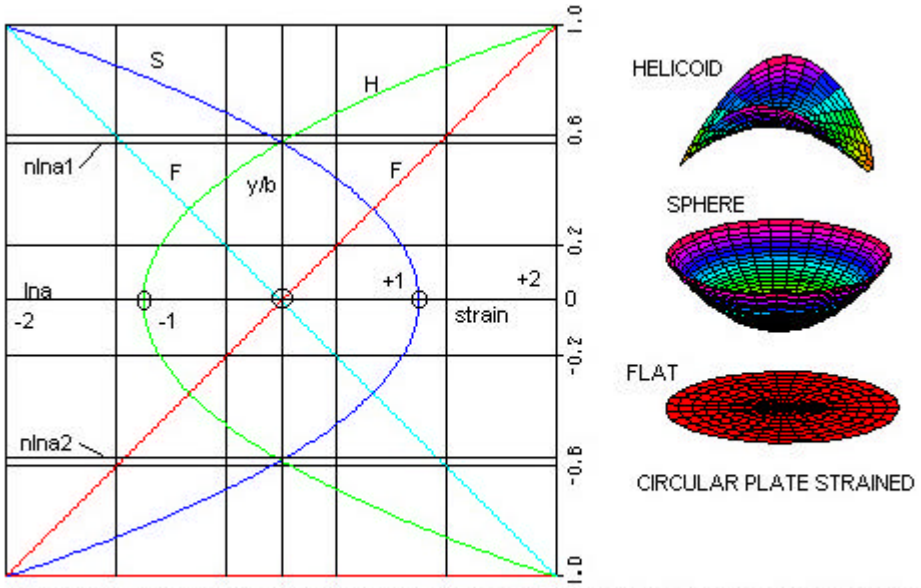

FIG 9. STRAIN DISTRIBUTION IN BENDING A STRIP TO A FLAT STRIP (F) BY LINEAR STRAIN, TO HELICOID (H) OR SPHERE (S) BY NON-LINEAR PARABOLIC VARIATION AROUND NUETRAL AXES LNA AND NLNA1 OR NLNA2

nonlinear parabolic strain distribution across the width. Three types of straining are possible. Let magnitude of strain at middle be ε_m Variation of strain $\varepsilon_x=\pm (Ky^2/2-\varepsilon_m)$,+ for helicoid, - for sphere set.. For helicoid straining, middle of strip (y=0) strain is $-\varepsilon_m$ compressive and at extreme fibers at $y=\pm(6\varepsilon_m/K)^{1/2}=2\varepsilon_m$ tensile. There is no longitudinal strain ε_x at $y=(2\varepsilon_m/K)^{1/2}$.ie Gaussian points. When sign of straining is reversed, i.e.,$\varepsilon_x= -(Ky^2-\varepsilon_m)$,we obtain a segment of a sphere set of constant positive K0. When the flat strip is strained linearly $\varepsilon_x=Ey/R$, K remains 0 as a developable surface, an annular ring segment, as in Engineer's Theory of Bending. Fig (9)

7.1 Stiffness and strength from stability

Stability of structures includes strength. *and* stiffness. Applying above stable construction, a computer model on NISA was generated using central pseudosphere design to replace a glass fiber reinforced plastic 720kg. vibration fixture with *steel* of same frequency , resulting in a design weight 175 kg.[7]. Using composites designed with stability principles as above, it is possible to effect an order of magnitude weight savings. We replace thick laminates by appropriately oriented reticulated beams for strength as well as stiffness

Bending twisting are together handled in isometry in isometry .It can find application in unsteady aerodynamics design to induce or suppress flutter of wings or FRP blades.

8.1 K inadequately recognized in design and analysis

Callidine [4], chapter 5,12 also refers to the relevance of K during inextensional deformations without explicitly mentioning Gauss Theorem or First fundamental form., but implicitly though Gauss-Codazzi relations of strain compatibility. He also decries the lack of emphasis of K , *" paradoxically, Gauss curvature is given little, if any, emphasis in text books"* in his textbook. The author of this paper is of the same opinion. Another pertinent comment by Den Hartog [5], page pp 319 relates to unexplained reduction in stiffness in bending, but increased stiffness in torsion of pretwisted strips. "*It is left as a challenge to the reader, in a subject as a old fashioned as strength of materials, new effects of considerable numerical importance can still be discovered in the atomic age*" .Implicit in stability is loading, static equilibrium and appropriate geodesy. This author's belief is strengthened or rather stiffened after investigations in isometry regarding its importance and long ignored rôle in structural stability and design.

9.0 STRUCTURAL ANALYSIS:

9.1 *Loading*

(a) Reticulated Pseudospherical Shell

A uniformly distributed compressive load is applied along the meridian of PS at its bigger and smaller ends. The axial force (along the height of the shell) is considered as 1kN.

(b) Continuous Composite Pseudospherical Shell

Load is applied through this skin at the smaller end

9.2 *Boundary Conditions*

(a) Reticulated Pseudospherical Shell

A symmetric boundary condition is applied at both ends of the PS.

(b) Continuous Composite Pseudospherical Shell

All six degrees of freedom are constraint in the bigger end of the PS**.**

9.3 *Material Properties*

(a) Reticulated Pseudospherical Shells

Material -Aluminum Alloy

Young's Modulus – 68.7MPa , Poission's ratio =0.3 and Yield stress = 350 N/mm^2

(b) Composite Continuous Pseudospherical Shell

Material- M55J/M18 carbon/epoxy

E_{11}= 328.95GPa, E_{22}=5.96GPa, G_{12}= 4.41GPa, ν_{12}= 0.346

9.4 *Finite Element Model*

An eight noded isoparametric quadrilateral shear flexible layered shell element is used for continuos composite shell type PS while a three node beam element with six degrees of freedom is used for reticulated type PS. It may be noted that PS synthesis

assumes infinitely small differential shell element length. However, in the finite element modeling distance between two grids which is defined as strut length has been arrived at based on Euler's column buckling load to eliminate the local buckling. NISA structural package was used for analysis.

Unlike the conventional continuous shell type structure, finite modeling of a reticulated pseudospherical shells is not straight forward. Initially, for central pseudosphere (③ = 1), cuspidal radius r_0=100 mm. Polar co-ordinates of the filament are (r,θ, z). θ varies from 30^0 to 90^0 with an increment of 3.75^0, and a spiral path with seventeen grids are generated using Eqns r = ro . sech θ , z = ro. (θ - tanh θ). Fibre angle -ψ symmetric to this is also generated. A total of 96 spiral paths ; 48 each at a polar angle interval of + 7.5^0 and – 7.5^0 respectively are created around the circumferential direction based on the above two basic paths. The netted paths are converted into three node beam elements with three translations and three rotations. Thus the total number of elements obtained are 1536.
In the case of continuous composite pseudospherical shell the nodes in the spiral paths are connected to form quadrilateral element. Five models of reticulated PS with different L/(R+r) aspect ratios and ranges of θ for PS segments are taken for the study. The details of geometric parameters are shown in Table-2.
The PS segment is generated by varying θ between π/6 to π. Minimum designs thickness at ψ = 30^0 is 1 mm. Thickness variation found by static equilibrium is
$⑨_s$ Area cos ❺ cos ❷ =const, Area=2πrt cos ❺ ,❷=❺, sin ❺/r=const, t/t_{30} = $.3248/(\cos^3\psi.\sin\psi)$

9.5 ANALYSIS RESULTS AND DISCUSSION
Deformed configurations of the five types of reticulated PS under static case is presented in Fig.(10.) and the buckling mode shape of PS with θ varying from 30^0 to 120^0 in Fig.(11).
Initially a convergence of the finite element is established for the reticulated PS with the medium mesh (with 1536 elements) and fine mesh (3072 elements). The net axial deflections in mm for the medium and refined meshes are obtained as 0.043 and 0.0431 respectively. Similar values for the radial deflections are obtained as 0.0631 and 0.063.
The superimposed deformed configuration of the pseudospherical shells presented in Fig.(10) for PS with various ratios of length to average diameter show that PS have reduced both in axial and radial directions retaining the overall shape of the shell. From the radial compression(deflection)given in Table-2, it can be observed that for the five different PS considered in the present study, same radial compression exists at planes of the same diameter. For instance, at a plane at locations B and C in this table, the radial compression are found to be 0.0283mm and 0.0173mm even for two different PS with θ=30^0 to 120^0 and 30^0 to 180^0 (model 2 and model 3). In general same radial compression can be seen at plane which contain same diameter even though there is wide variation of θ range used in configuring a PS segment the range of θ varies for PS is different. Such a behavior is possible only when a pure membrane state of stress exists with stability for this class of structure. This is also verified from the top and bottom fibre stresses of the reticulated structure
The critical buckling stress in the PS is found to increase from 508.2 N/mm^2 to 1160.5 N/mm^2 as the aspect ratio L/(R+r) increases from 0.48 to 4.46 contrary to what one

would expect as an Euler column. The buckling load of PS is expected to be independent of aspect ratio. This unconventional result of the PS can be attributed to the typical negative Gauss curvature and stable filament path by which it possesses a state of membrane stress along its length. It can also be observed that a PS with $\theta = 90^0$ to 180^0 and 120^0 to 180^0 have significant load bearing capabilities than a PS with $\theta = 30^0$ to 90^0, $\theta = 30^0$ to 120^0 and $\theta = 30^0$ to 180^0. In a given PS whatever may be the curvature the stress experienced by a given strut (length between two junctions) remains same. The entire shell shortens like a short strut. It may be noted that the structure does not undergo any local buckling as polar symmetry and similarity to unloaded structure are maintained in the buckled mode. Because of this important and characteristic nature of the reticulated PS, the design of the same is independent of the overall size but depends upon local strut length between nodes.The buckling mode is of a global character, without loss of local similarity to original structure at any point .This important rigid mode is to be noted.

In the case of a composite continuous pseudospherical shell, the critical buckling stress is obtained as 600 N/mm^2 as against its unidirectional compressive strength of 720 N/mm^2. The deformed configuration of the shell under static load is found be geometrically similar to the original configuration as observed in the case of the reticulated shells.

TABLE – 2 Displacements and Critical Buckling Stresses in Reticulated Pseudospherical Shell Segments

Model No.	Polar angleθ	Truncated Shell Size (mm)	Aspect ratio L/(R+r)	θ values at start, middle,and end of PS (in degrees)	Radial displacements at corrosponding locations (in 0.1mm)	Critical Stress (N/mm^2)
1.	30^0 to 90^0	L= 61 R= 88 r = 40	0.48	30,90	0.631, 0.282	508.2
2.	30^0 to 120^0	L= 108 R= 88 r = 24	0.96	30,60,120	0.631,0.283,0.173	709.9
3.	30^0 to 180^0	L= 210 R= 88 r = 8.6	2.18	30,90,120,180	0.631,0.283, 0.173, 0.061	739.3
4.	90^0 to 180^0	L= 149 R= 40 r = 8.6	3.07	90,120,180	0.283,0.173,0.061	927.0
5.	120^0 to 180^0	L= 102 R= 24 r = 8.6	4.46	120,180	0.173, 0.061	1160.5

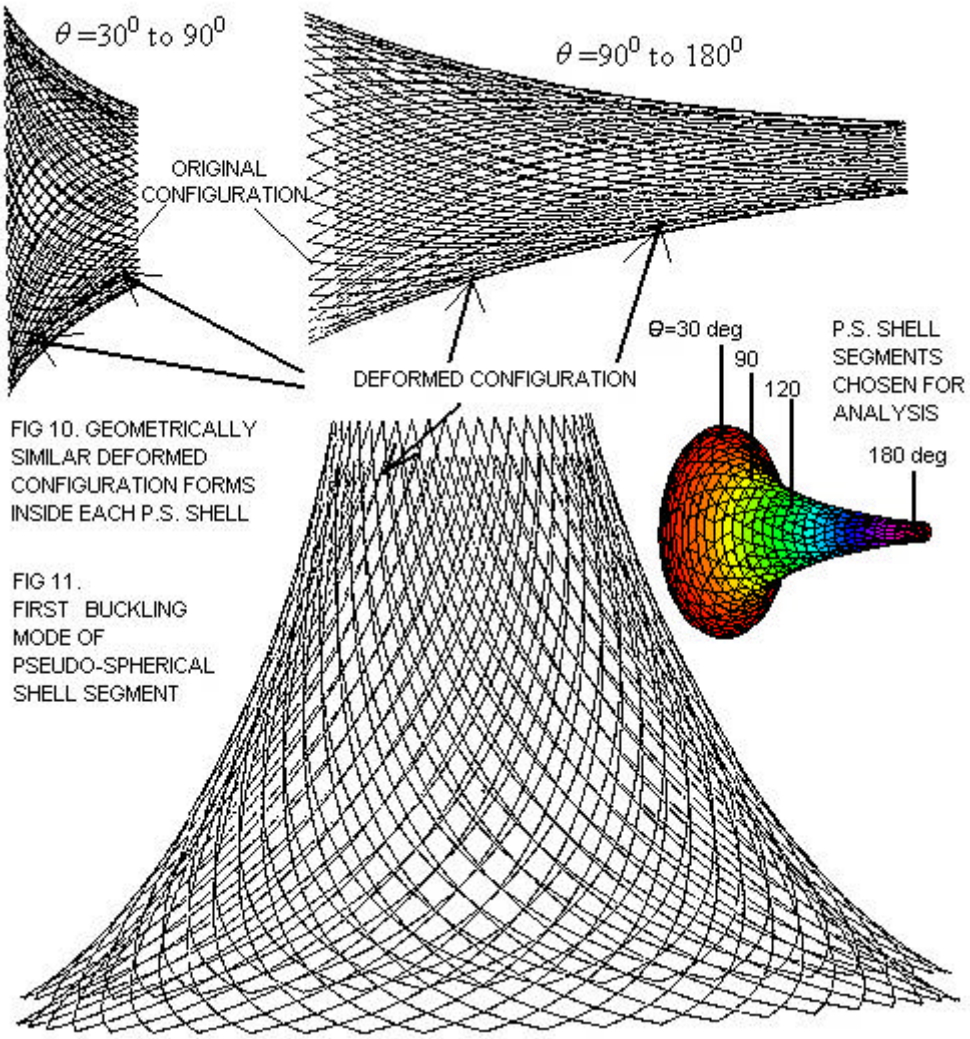

FIG 10. GEOMETRICALLY SIMILAR DEFORMED CONFIGURATION FORMS INSIDE EACH P.S. SHELL

FIG 11. FIRST BUCKLING MODE OF PSEUDO-SPHERICAL SHELL SEGMENT

CONCLUSIONS

Classical theory of isometric mapping or deformations has been interpreted and applied for structural bending. A model in hyperbolic geometry using polar coordinates has been constructed. Hyperbolic geodesics are given as essential buckling resisting stable directions and are seen to agree with Egregium theorem as isometric bending invariant. Generalized Mohr circles for depicting isometric bending deformations and geometrical direct and inverse isometry of two types are introduced in this paper. Importance of Gauss curvature in large shell membrane strain is pointed out. .A pseudospherical shell has been structurally synthesized. This has been demonstrated to proceed directly, apparently without any bifurcation, to compressive failure without buckling, confirmatively established by finite element analysis.

ACKNOWLEDGEMENTS

The authors record profound gratitude for understanding and encouragement shown during expression of this new theoretical theme for structural application from our senior colleagues of Vikram Sarabhai Space Center Dr. S.Srinivasan, Shri Rajaram Nagappa, Dr.G.V.Rao, and Shri M.Ramakrishnan.The first author gratefully remembers exhortation from former colleague Shri C.R.Sathya , to “put it down”.

REFERENCES

1. Roborto Bonola, *Non-euclidean geometry* Dover Publishers, NY, 1979.
2. Dirk. J. Struik, *Lectures in classical differential geometry,* Dover Publishers, NY, 1988, pp 121.
3. Heinrich W. Guggenheimer, *Differential geometry,* Dover Publishers, NY, 1977.
4. Callidine C.R,. *Theory of shell structures,* Cambridge University Press,1968.
5. J.P. Den Hartog , *Advanced Strength of Materials,* Dover Publishers, NY, 1983.
6. Anoop Abraham, J.P.Jacob,Riju Abraham, Shihad V.M., *Static and Buckling characteristics of pseudospherical shells* , Project Report, R.G. Institute of Technology, Mahathma Gandhi University, Kottayam , B.Tech Project Report. 1997.
7. Baiju Sasidharan, *Design, Analysis and Fabrication of a Pseudospherical Shell as a Vibration Test Fixture*, Master of Technology Thesis Report, Dept. of Ship Technology, Cochin University of Science and Technology, 1998.
8. Karl Friedrich Gauss, *Disquisitiones generales circa superficies curvas 1827* (Werke 4, pp 217 – 258).